Article

Charge-directed Immobilization of Bacteriophage on Nanostructured Electrode for Whole Cell Electrochemical Biosensors

Yan Zhou, Abhijit Marar, Peter Kner, and Ramaraja Pandian Ramasamy

Anal. Chem., **Just Accepted Manuscript** • Publication Date (Web): 09 May 2017

Charge-directed Immobilization of Bacteriophage on Nanostructured Electrode for Whole Cell Electrochemical Biosensors

Yan Zhou[a,b] , Abhijit Marar[c], Peter Kner[c] and Ramaraja P. Ramasamy[a,b*]

[a] Nano Electrochemistry Laboratory, School of Chemical, Materials and Biomedical Engineering, University of Georgia, Athens, Georgia 30602, USA

[b] Department of Chemistry, University of Georgia, Athens, Georgia 30602, USA

[c] School of Electrical and Computer Engineering, University of Georgia, Athens, Georgia, 30602, USA

*E-mail: rama@uga.edu, Fax: +1-706-542-3804

Abstract:

A new type of carbon nanotube (CNT)-based impedimetric biosensing method has been developed for rapid and selective detection of live bacterial cells. Proof of concept study was conducted using T2 bacteriophage-based biosensors for electrochemical detection of *Escherichia coli* B. The T2 bacteriophage (virus) served as the bio-recognition element, which was immobilized on polyethylenimine (PEI)-functionalized carbon nanotube transducer on glassy carbon electrode. Charge-directed, orientated immobilization of bacteriophage particles on carbon nanotubes was achieved through covalent linkage of phage capsid onto the carbon nanotubes. The presence of the immobilized phage on carbon nanotube modified electrode was confirmed by fluorescence microscopy. Electrochemical impedance spectroscopy (EIS) was used to monitor the changes in the interfacial impedance due to the binding of *E. coli B* to T2 phage on the CNT-modified electrode. The detection was highly selective towards the B strain of *E. coli* as no signal was observed for the non-host K strain of *E. coli.* The present achievable detection limit of the biosensor is 10^3 CFU/mL.

Keywords: Electrochemical Biosensor, Bacteria Detection, Charge-directed Immobilization, Electric field-induced Immobilization, Electrochemical Impedance Spectroscopy.

Introduction

Bacterial pathogens are universally present in the environment and are important targets for detection and identification in various applications, such as food safety,[1,2] environmental pollution and public health.[1,3] It is important to develop accurate and robust technologies for identification and detection of bacteria in complex matrices. Conventional methods for bacterial identification includes standard microbiology or biochemical procedures, such as culture and cell counting of bacteria, enzyme linked immunosorbent assay (ELISA) and polymerase chain reaction (PCR), etc. While being highly reliable, these methods are also laborious, time-consuming, typically expensive, and require laboratory set up, rendering them unsuitable for rapid screening purposes by an unskilled user outside the laboratory set up.[4] Biosensors are advantageous in this respect, as they are simple, easy to use, and provide rapid response for real time monitoring purposes. Biosensors are devices that incorporate a biological recognition element with high specificity towards target analyte(s). A typical biosensor consists of three components, bioreceptor (enzyme, protein, antibody, DNA and even viruses), transducer element and data processing unit.[4,5] Typically, biosensors can be categorized by the type of bioreceptors, or by the mode of transduction. The transduction mode could be optical, piezo-electric or electrochemical. Electrochemical biosensors are of particular interest because of their simplicity, fast response and high sensitivity.[6-8] The specificity and cost of an electrochemical biosensor is highly dependent on the type of the bio-recognition element being used, such as enzymes, antibodies, DNA/RNA, aptamers or bacteriophages.[9] While aptamers, antibody and enzymes possess high selectivity, they are highly susceptible to damage or loss of activity in harsh environmental conditions for bacterial cell detection. DNA-based detection methods could not distinguish viable cells from dead cells and require rigorous sample processing.[10] On the other hand, bacteriophage (or simply phage) viruses are inexpensive, ubiquitous in nature, possess robust stability under sub-optimal environmental conditions. As a bio-recognition element, bacteriophages offer high selectivity towards their host bacteria and could discriminate between

viable and nonviable cells. A phage could recognize its host bacterium through the bacterial surface receptor, followed by binding onto the bacterial cell. Upon attachment, the phage penetrates the bacterial cell membrane and injects its genetic material (DNA/RNA), which initiate protein synthesis, phage assembly and replication inside the bacterium. This leads to the bacterial cell lysis (break open) and the release of new virus particles. The mechanism reflects a recognition system in which phage particles specifically recognize and bind only to their host bacterial cells and not towards other cells. Thus, bacteriophages represent ideal choice as bio-recognition element for biosensors for bacterial cell detection.[11,12]

An electrochemical biosensing method utilizing phage as a bio-recognition element for whole cell bacteria detection could be developed by immobilizing phage particles on electrode surfaces. The use of nanostructured electrodes for phage immobilization further enhances the sensitivity of electrochemical detection. Towards this end, various approaches have been proposed to immobilize phage on electrochemical biosensor platforms, from a simple physisorption to covalent crosslinking.[13-17] Much of the efforts in the published literature have been focused on increasing the number of surface phage particles per unit area for signal enhancement purposes, in which the phage was randomly oriented on the surface for either amperometric-based electrochemical biosensor, or surface plasmon resonance-based optical biosensor construction.[11,17-19] Since 95% of bacteriophages isolated to date are tailed and possess asymmetric shape, it is important to achieve the desired orientation of phages on the transducer surface to function effectively as a bio-recognition element.[20,21] For *Myoviridae* phages, that contain a distinct head (capsid)-tail structure such as the T4 phage, it is important to orient the phage in a manner that all the capture proteins (tail fiber) are exposed to target the host bacterial cells. However, a vast majority of the published literature on phage-based biosensors, do not address this problem satisfactorily. Asymmetrical phage particles immobilized on biosensor surface without a preferred orientation generally exhibit low bacteria capture efficiency as shown

by Hosseinidoust *et al.* for T4 towards the capture of *E. coli* cells.[22] This underscores the importance of oriented immobilization of phage on electrode surface for biosensing purposes.

Most attempts reported in the literature for attaching phage to a surface were based on a recombinant engineering of phage capsid proteins, such as biotinylation of phage head proteins which immobilize phage in capsid down – tails up fashion.[12,21] There have also been reports about oriented phage immobilization on surfaces without recombinant engineering.[23-25] Most phages have net negative charge, with a negatively charged capsid (head) and positively charged tail fibers. This charge difference between the head and tail fibers of the phage could be utilized for immobilizing phage on electrode surface using electrostatic interaction and electrophoretic deposition. For example, H. Anany *et al.* proposed a method for the oriented immobilization of bacteriophage on positively charged cellulose membrane that attracts large number of phage particles to its surface due to their net negative charge.[23] Han *et al.* proposed the capture of T7 bacteriophage on an indium tin oxide surface through electrophoresis for virus detection. The electrophoretic trapping of phage particles offers a simple method to achieve a controllable array of phages in the correct orientation.[24] Richter *et al.* studied the behavior of phage upon aligned along the electric field and applied the phage-modified substrate for flow cytometry.[25]

In this work, we report our work on the development of an electrochemical biosensing method for bacterial cell detection using phage as a bio recognition element. Here we attempted an electric field-induced (EFI), charge-directed orientation strategy for immobilizing bacteriophage on carbon nanotube modified electrode surface for electrochemical detection of bacterial cells. Using this immobilization method, a novel T2 bacteriophage-assisted carbon nanotube-based impedimetric biosensor was developed for *E. coli* detection, in which the T2 was immobilized on cationic polymer functionalized multiwall carbon nanotube (CNT) electrodes. T2 phage contains negatively charge on the capsids (heads) and positively charged on the tail fibers. Using electric field-induced immobilization, T2 phages could be oriented on positively charged functionalized CNT matrices to enable the chemical anchoring of phage onto the

nanostructured electrode. The resulting T2 phage-modified CNT electrodes were used as biosensors for the detection of *E. coli B* using electrochemical impedance spectroscopy as the detection technique.

Experimental section

Materials and instruments

The following chemicals were purchased and used without further purification: sodium chloride and sodium phosphate dibasic (both from EMD chemicals), potassium dihydrogen phosphate (BDH), magnesium sulfate heptahydrate (J.T. Baker), 1-pyrenebutanoic acid succinimidyl ester (PBSE) (Sigma Aldrich), polyethylenimine (PEI) (Sigma Aldrich), yeast extract and agar powder (all from Alfa Aesar), tryptone (Amresco). Multi-walled carbon nanotubes (CNT) (diameter 8-15 nm) was obtained from Cheap Tubes Inc. SM buffer was prepared by mixing 5.8 g of NaCl, 2 g of $MgSO_4 \cdot 7H_2O$, 50 mL of 1M Tris-HCl pH 7.5, and 1 mL of 10% (w/v) gelatin in deionized water. Luria-Bertani (LB) medium was prepared by mixing 10 g of tryptone, 5 g of yeast extract and 10 g of NaCl in deionized water and adjusted to pH 7.0. LB-agar medium was prepared by adding 6 g of agar to 400 mL of LB media. 2 g of agar was added to 400 mL of LB media to obtain soft agar medium. 10X phosphate buffered saline (PBS) was prepared by mixing 16 g NaCl, 0.40 g KCl, 2.8 g Na_2HPO_4, and 0.49 g KH_2PO_4 in 200 mL deionized water yielding a buffer solution of pH 7.4. The prepared PBS was further diluted to 1X before use. All media, buffer and glassware were sterilized before use. *E. coli* B and T2 phage were purchased from ATCC (11303 and 11303-B2, respectively). *E. coli* K strain was kindly provided by Dr. Yajun Yan (University of Georgia, Athens). Glassy carbon electrode (GCE) obtained from CH Instruments was used for all electrochemical experiments (3 mm diameter).

Scanning electron microscopy (SEM) images of the modified electrode were obtained using FEI Inspect FEG electron microscope. Attenuated Total Reflectance-Fourier transform infrared

spectroscopy (ATR-FTIR) measurements were performed on carbon nanotube coated silica wafer in Nicolet 6700 instrument. Fluorescence images were obtained using EVOS fluorescence microscopy (Invitrogen). Surface charge of carbon nanotubes, bacteria and phage particles were analyzed by ZetaSizer (Malvern). Contact angle measurements to determine hydrophobicity of the CNT electrodes before and after PEI functionalization were performed by a KrüSs DSA 100 using a 1 μL drop of 18 MΩ water (pH 7).

Bacteria preparation and phage propagation

E. coli B (ATCC 11303) were grown in 4 mL of LB medium overnight at 37 °C. 1 mL aliquot of the overnight culture was inoculated into 100 mL of fresh LB, followed by incubation for 3 h at 37 °C in an incubator shaker. 1 mL of the culture was then centrifuged at 4000 g for 10 min to remove medium and washed with 1X PBS buffer for twice before each experiment. Enumeration of bacteria was performed by plate count techniques and expressed in CFU/mL. T2 bacteriophage (wild type) was amplified using soft agar overlay techniques (see detailed method in the Supporting Information). Plaque assay was applied to measure the phage titer and was expressed in PFU/mL prior to use.

Phage immobilization and electrode preparation

Multiwall carbon nanotubes (CNT) was functionalized with polyethylenimine (PEI) to obtain positive surface charge as previously reported (See detailed method in the Supporting Information).[26] To facilitate phage immobilization onto CNT modified electrode surface, a positive potential was applied on working electrode for phage deposition, followed by covalent linkage of phage through PBSE onto PEI-*f*-CNT (see Scheme 1). Glassy carbon electrode was used as working the electrode and was modified using the following procedure: 2 mg of PEI functionalized multiwall carbon nanotube (PEI-*f*-CNT) was dispersed in 1 mL deionized water. The suspension was ultra-sonicated for 10 min prior to use. 12 μL PEI-*f*-CNT was dropcast on glassy carbon electrode (GCE) surface and dried. Prior to phage attachment, the PEI-*f*-CNT modified GCE was activated with succinimidyl ester (PBSE) as molecular tethering agent. For

this, 4 μL of 10 mM PBSE solution (in DMF) was dropcast on the PEI-*f*-CNT modified GCE electrode and allowed to react for 15 min on ice. The excess unreacted PBSE was removed by rinsing the electrode with DMF, followed by PBS buffer. [27-31] For electric field-induced immobilization, a positive potential of +0.5 V *vs* Ag/AgCl was applied to the working electrode for 1h in a 1X phosphate buffer solution (PBS) containing bacteriophage (~10^9 PFU/mL) in order to facilitate the charge-directed immobilization process. Finally, the phage immobilized electrode was rinsed using SM buffer and covered with 50 μL *E. coli* B suspension for 30 min. After *E. coli* incubation, the electrode was rinsed with buffer and was used to perform electrochemical impedance measurements. For control experiments, the biosensor was tested in the buffer without bacteria (negative control) and in the buffer with non-host *E. coli* K strain (positive control). Seven-fold serial dilutions (10^2-10^8 CFU/mL) of *E. coli* B were prepared for bacterial cell detection experiments.

Fluorescence imaging of bacteria and phage

To characterize the surface immobilized phage, 100 μL of phage solution (10^{10} PFU/mL) was stained with SYBR gold, a fluorescent nucleic acid dye with EX/EM of 495 nm/537 nm, at a final concentration of 5X for 20 min at room temperature. Free dye was removed by centrifugation (see detailed method in the Supporting Information).[32] Phage was then added to electrochemical cell for electric field-induced immobilization using CNT coated ITO glass slide as working electrode. The reason for using the ITO glass slide as electrode instead of GCE is due to the practical difficulties in accommodating the rod shaped GCE inside the fluorescence microscope. Same experimental procedure as mentioned earlier for GCE was used to immobilize phage onto ITO surface in dark. The resulting ITO was used for fluorescence characterization (see detailed method in the Supporting Information).[33]

Infectivity of immobilized phage

Phage immobilized CNT coated ITO glass slide was prepared using the same method to study the infectivity of the immobilized phage. The infectivity of the immobilized phage was verified

using the disk diffusion technique as reported elsewhere.[34] The agar plates were topped with cut-out electrode discs immobilized with phage particles. The agar plates were inspected on the subsequent day for lysis rings around the electrode disks. ITO glass slides with no phage were used as a negative control.

Electrochemical characterization

Electrochemical characterization was conducted using CHI-920c model potentiostat (CH Instruments Inc, Austin, TX). A conventional three-electrode cell (a working electrode, an Ag/AgCl reference electrode and a Pt wire auxiliary electrode) was used for electrochemical measurements. All the electrochemical measurements were carried out at 25 ºC ± 2 ºC in a 5 mL voltammetry cell containing 5 mM $Fe(CN)_6^{3-/4-}$ (1:1) mixture in 1X PBS buffer, unless otherwise stated. Impedance was measured at the open circuit potential, with a superimposed AC voltage of amplitude 5 mV between frequencies 100 kHz and 10 Hz.

Results and Discussion

Characterization of PEI-functionalized CNT

Successful functionalization of PEI on CNT was verified using ATR-FTIR measurements of the modified electrode to study the characteristic peaks of the functional groups on the CNT surface. The resulting ATR-FTIR spectra are shown in Figure 1. The presence of amide bond due to PEI functionalization of CNT was confirmed by C=O adsorption at 1690 cm^{-1}. The O-H group resulting from the acid treatment of CNT was observed at 3440 cm^{-1}. In addition, two absorption peaks at 2931 and 2854 cm^{-1} in the spectra could be assigned to CH_2 stretching in the alkyl chain of PEI. Meanwhile, adsorption due to CN stretching was identified at 1370 cm^{-1}. The identification of these peaks confirmed the successful functionalization of CNT with PEI based on the literature.[35]

Figure 2 shows the SEM images of CNT before and after PEI modification differentiating the morphology of the nanostructured electrode before and after cationic polymer

functionalization. Some aggregation of CNT occurred after PEI functionalization of CNT with formation of many mesopores as shown in the Figure 2. The surface amine functional groups increased the surface energy on CNT and made the surface more hydrophilic resulting in the low contact angle of 29° (see inset in Figure 2) for contact between water droplet and the CNT coated surface. On the other hand, the surface functional groups also altered the surface charge and the zeta potential of CNT. The zeta potentials of CNT, PEI-*f*-CNT in pH 7.4 PBS were -20.2 ± 0.7 mV and +12.4 ± 0.8 mV, respectively. Positively charged PEI-*f*-CNT hence prepared was used as for the immobilization of negatively phage particles in further studies.

Characterization of immobilized bacteriophage

Zeta potential measurements elucidate the surface charge and colloidal stability of biological particles. The zeta potential of T2 phage in PBS buffer was measured as -10.0 ± 0.8 mV, resulting in a net negative charge.[23] However the charge distribution varies along the length of the phage with the capsid being more negatively charged and the tail being more positively charged.[23] *E. coli* (ATCC 11303) has zeta potential of -9.7 ± 1.1 mV. In order to achieve the highest capture efficiency of bacteria with immobilized phage particles, T2 phage particles should be immobilized with its positively charged tail-spike proteins exposed to negatively charged bacterial cells. The heads down-tail up fashion of phage on the electrode would help orient the phage towards bacterial cell capture by the exposed tail fibers and this orientation is facilitated through PEI functionalization of CNT and subsequent electric field-induced immobilization of phage onto PEI-CNT. As previously discussed, the electric field-induced immobilization described in the Scheme 1 uses the hetero-bifunctional molecular tethering agent PBSE for establishing covalent linkage between the phage and the PEI-*f*-CNT. The aromatic pyrene moiety of the PBSE interacts with CNT side walls through π-π stacking as demonstrated in our previous work,[27,29,31,36,37] while NHS ester moiety binds with primary amine groups in the surface proteins (of T2) to form amide bonds. The PBSE based molecular tethering method has been demonstrated before for enzymes and bacterial cells, but never has been explored before for

tethering viruses on CNT.[27] For phage immobilization, the electric field was induced by applying a potential of +0.5 V *vs* Ag/AgCl to the PEI-*f*-CNT electrode for 1 h using 10^9 PFU/mL phage solution. During electric field-induced immobilization, an electrical double layer could form in the proximity of electrode surface on which the phage is deposited (Scheme 1). The formation of this negative ion layer may decrease the intensity of the electric field inside the electrolyte, resulting in disorientation of phage particles. The orientation of the phage particle are related with Debye length (κ^{-1}) on the CNT surfaces.[25] The phage particles will align along the lines of the electric field within the small volume when κ^{-1} is larger than the size of the phage. When κ^{-1} is smaller than the size of phages, the orientation of the phage particles occurs due to electrostatic interaction.[38,39] In our case, T2 phage is much larger than typical κ^{-1} (few nanometers). Thus, it can be concluded that the immobilized phages were preferentially attached on to the CNT modified electrode in head down-tail up orientation as described in Scheme 1.

To further visualize bacteriophage on electrode surface, T2 bacteriophage were labeled using a DNA intercalating SYBR Gold dye. An electric field was applied as mentioned previously to the PEI-*f*-CNT electrode. The covalent linkage between phage and the CNT is formed by the PBSE as described above. The resulting fluorescence images of the immobilized phages are shown in Figure 3. The images in Figure 3a-b confirm a successful immobilization of bacteriophages onto PEI-*f*-CNT using electric field-induced, charge directed immobilization method. About 140 phage particles were observed on a matrix size of 16 μm ×16 μm. Control experiment for phage immobilization without electric field (no voltage applied) resulted in only 9 phage particles on the PEI-*f*-CNT as shown in Figures 3c-d. No phage particles were observed in the negative control (in the absence phage) in Figure 3e. The fluorescence seen in Figure 3e is due to the autofluorescence of the CNTs which is well established in the literature and therefore should not be confused with that of the fluorescence from phage particles.[40] The higher intensity of the CNT in Figure 3e can be explained due to the higher intensity used while imaging (343 vs. 114 W/cm^2) and also from the fact that the substrate in Figure 3e was aligned in the focal plane

as opposed to Figures 3a-d where the CNT were out of focus. From these results, it can be concluded that the electric field-induced immobilization methods results in 15 X higher loading of phage particles on the electrode surface, ensuring high bio-receptor loading on the electrode surface for host bacterial cell detection.

Since there is no feasible and reliable method for estimating the number of the receptors on the electrode surface, the activity of the immobilized phages was verified for their infectivity using disk diffusion method.[34] This infectivity study requires a flat electrode and therefore CNT-coated ITO glass was used as working electrode for this purpose. The ITO electrode was further incubated on a lawn of bacteria using soft agar overlay method. As shown in Figure S1a (see Supporting Information), lysed rings up to 1 mm thick were found around the ITO electrode with immobilized phages, whereas ITO electrode without phage in Figure S1b showed no such lysis rings around the electrode. The results indicate that the immobilized phages were able to lyse (kill) bacteria cells and were thus deemed active and infectious. The T2 phage modified PEI-*f*-CNT nanostructured electrode was then evaluated as a biosensor for the detection of *E. coli* B using electrochemical impedance spectroscopy.

Electrochemical characterization and bacteria detection

Electrochemical impedance spectroscopy (EIS) was used to further characterize the assembly of the biosensor in a PBS (pH 7.4) containing 5 mM $Fe(CN)_6^{3-/4-}$ as the redox couple. EIS was reported as an effective and non-destructive method to monitor electrode surface characteristics. In the presence of $Fe(CN)_6^{3-/4-}$, the impedance measured is the Faradaic impedance of the redox couple.[4] Supplementary Figure S2 (see supporting information) illustrates the results of Nyquist plot ($-Z_{im}$ *vs* Z_r) of bare PEI-*f*-CNT and phage modified PEI-*f*-CNT in the presence of 5mM $Fe(CN)_6^{3-/4-}$ redox couple in PBS (pH 7.4). The results show that electric field-induced (EFI) immobilization of phage achieved higher loading of phage particles (as measured by the largest variation in the R_{CT} of the electrode upon phage immobilization) on the electrode surface compared to non-EFI immobilization. This observation is consistent with

the results of the fluorescence images. The high phage loading on CNT could help to enhance the biosensor performance as evaluated and discussed below.

Figure 4a illustrates the representative open circuit Nyquist plots measured using the phage-modified nanostructured electrodes for the 5mM $Fe(CN)_6^{3-/4-}$ redox couple obtained both in the absence and presence of bacteria (at different concentration expressed in CFU/mL) in the electrolyte solution. The equivalent electrical circuit, also called Randles circuit, used to fit the Nyquist data is also shown as an inset in Figure 4a. This model consists four circuit elements, including the electrolyte resistance (R_Ω), charge transfer resistance (R_{CT}), double layer capacitance (C_{dl}), and Warburg impedance (Z_w). Among them, R_Ω and Z_w represent the ohmic resistance of the electrolyte solution and the mass transfer impedance for the diffusion in and out of the redox couple from electrolyte bulk to the surface, respectively. C_{dl} represents a nonideal capacitance at the electrochemical interface. The arc of the Nyquist plot reflects the charge transfer resistance R_{CT}, which is determined by the type of surface modification and the kinetics of the redox reaction. The capture of bacterial cells on phage-modified electrode surface could alter the surface properties of electrode which in turn vary the impedance measured on the biosensor electrode.

To evaluate the sensitivity of the biosensor, the phage-modified nanostructured CNT electrode was used for the detection of *E. coli* B from its suspensions of different concentrations (10^2-10^8 CFU/mL). The bacterial cell suspensions were incubated on the phage-modified electrode surface then rinsed before the AC impedance measurements. Impedance measurements were made at different *E. coli* B concentrations and the results were compared with that of the control where no *E. coli* was present. As shown in Figure 4a, the diameter of the Nyquist arc decreased with increasing bacterial cell concentrations suggesting a direct influence of bacterial cell attachment on the impedance of the above redox reaction. As expected, a significant variation was observed in R_{CT} upon the *E. coli* attachment onto phage modified nanostructured electrodes, and the difference is amplified at high *E. coli* concentrations (see magnitude of the

arc in Figure 4a). Table S1 shows the fitted data of parameters such as R_{Ω} and C_{dl}. A considerable decrease of charge transfer resistance was observed after 30 min contact between surface immobilized phage and *E. coli*. In many impedimetric biosensors, charge transfer resistance usually increases with increasing *E. coli* concentration.[41-44] Such increase in R_{CT} due to *E. coli* attachment could be attributed to the lowering of redox kinetics at the interface, as *E. coli* could act as a barrier on the electrode blocking the accessible CNT sites for $Fe(CN)_6^{3-/4-}$ redox reaction.

In order to completely understand the relation between charge transfer resistance and surface attached bacterial cells, a live/dead cell viability assay was performed to study the interaction between bacteria cells and surface immobilized phage particles. According to the fluorescence images shown in Figure 5, the immobilized T2 was seen to disturb the integrity of the cell membrane with increasing incubation time. The images in Figure 5 show a progressive decrease of green fluorescence (viable *E. coli* cells) and increase of red fluorescence (dead *E. coli* cells) due to phage infection. A distinct variation in the number of viable *E. coli* cells was noticed after 20 minutes and the cells were completely compromised after 25 min, suggesting the infection time of *E. coli* and the lytic cycle of immobilized phages was around half an hour. It is reasonable to assume all *E. coli* cells that remained on the electrode surface were attached to phage particles. However, not all bacterial cells were compromised at the same time. The released phages from lysed cells may further infect surrounding bacterial cells resulting in increasing number of red fluorescence over longer periods of time. Above all, immobilization of phages onto electrode surface shortened the latent period of phage. The fluorescence study also indicated that the electrochemical measurements were conducted during the lysis of bacterial cells.

In the present electrochemical impedance measurements, the subsequent decrease of charge transfer resistance happens presumably as the consequence of phage infection and bacterial cell lysis. Following the lysis of bacterial cells, progeny phages could be released and induce more

disruption of cell walls and release of intracellular components. As observed by Shabani and Mejri, the released intracellular components may increase the surrounding medium conductivity at the electrode surface which contributes to the decrease of charge transfer resistance.[15,45] As shown in Table S1, R_{CT} decreases with increasing number of bacteria cell concentration. Correspondingly, the values of C_{dl} at different bacterial concentrations shows a 40% increase in the double layer capacitance of the electrode at high bacterial concentrations. The slight increase of double layer capacitance (from 10^4 to 10^6 CFU/mL) may result from the increase of dielectric permittivity caused by higher number of bacterial cell lysis. Given that phage latent period would be shortened after surface immobilization, with high concentration of bacterial cells binding onto electrode surface, cell lysis may happen simultaneously on the electrode surface. More phages will be released and induce further infection of surrounding bacterial cells. This chain of events will contribute to greater amount and faster release of intracellular ions in the form of cell lysate, which could influence the electrical double layer thickness and in turn influence the charge transfer resistance.[15] On the contrary, when only few bacterial cells bind to the electrode surface, the cell lysis may not have huge impact on surrounding bacterial cells and the charge transfer resistance. This effect was observed in Table S1 for low bacterial cell concentrations (10^2-10^3 CFU/mL). Figure S3 represents our hypothesis for the above argument. However further studies are needed to better understand the role of the intracellular ions during cell lysis on the interfacial impedance of the electrode.

A linear correlation between R_{CT} and the bacterial concentration was observed between 10^3 and 10^7 CFU/mL as shown in Figure 4b. No significant variation in R_{CT} was observed for concentrations below 10^2 CFU/mL in a 50 µL *E. coli* suspension. At and above bacterial cell concentrations of 10^7 CFU/mL, the change in charge transfer resistance is insensitive to changes in cell concentration, which may be due to surface saturation of adhered cells. The lowest concentration that can be determined to be statistically different from a blank (noise) is considered as the limit of detection (LOD) of the sensor. The LOD is recommended to be a

measurement level of 3σ units above the value of blank, where σ is the standard deviation of the blank.[46] The LOD was calculated from the slope of calibration curve according to the following equation: LOD = kσ/m, where k = 3, σ = standard deviation of blank, and m = slope of calibration curve. The calculated LOD is 10^2 CFU/mL which resides below the linear range, where calibration curve is no longer valid. Therefore, in order to define the smallest concentration of bacteria that can be detected, we used k = 5 for LOD calculation in order to provide a more conservative estimation of LOD. The detection limit of the biosensor hence determined was 1.5×10^3 CFU/mL in a 50 μL *E. coli* volume. For control experiment, the same set of detection experiments were performed using bare PEI-*f*-CNT electrodes (without phage) to identify non-specific adsorption of *E. coli* cells as shown in Figure 4b. A comparatively minor R_{CT} variation was observed over the same concentration range.

The sensitivity of bacterial detection by phage-based biosensor could be influenced by the type of immobilization method used for attaching phage to the electrode surface as reported in the literature.[11,15-19] In the present study, the phage-based biosensor achieved a detection limit of 10^3 CFU/mL for *E. coli* B, which is better than most impedimetric sensors reported before.[41-44] Bacteriophages were treated as charged particles which could be immobilized onto working electrode. By electric field-induced alignment, a high loading of phage particles could be immobilized through charge directed orientation and covalent attachment. More importantly, the surface cationic polymer modified CNT interacts with negatively charged phage capsid followed by PBSE-based covalent linkage, leading to oriented immobilization and higher bacteria capture efficiency. As a result, the electric field-induced immobilization of phage particles could in turn affect the overall biosensor sensitivity.

Selectivity of the phage-based impedimetric biosensor:

To evaluate the specificity of the T2 phage towards the B strain of *E. coli*, the biosensor was tested using non-host control bacteria *E. coli K* strain (at 10^3~10^6 CFU/mL,). As shown in Figure S4 (see supporting information), no plaques were observed after incubating T2 phage with K

strain *E. coli*. When evaluated electrochemically using impedance, similar conclusion could be reached. Figure 6a shows the Nyquist plots of T2 phage-modified electrodes in the absence and presence of B (native host) and K strains (non-host) of *E. coli*. Figure 6b shows the variation in R_{CT} upon increasing bacterial concentrations. The figure shows little to no variation in charge transfer resistance for the K strain compared to the B strain, clearly demonstrating the biosensor is non-responsive to the non-host *E. coli* K strain. The results demonstrate that the phage-biosensor is highly specific only to the target host strains of the bacterial species.

Conclusion

We have demonstrated a new approach for whole cell bacteria detection using bacteriophage-assisted CNT-based electrochemical biosensor. A reliable method for oriented immobilization of bacteriophages on CNT was developed by combining electric field-induced, charge-directed immobilization and covalent crosslinking. Bacteriophage particles was deposited with tail up and capsid down orientation, followed by covalent binding onto PEI-functionalized CNT sidewall through molecular crosslinkers. This new approach offers a high loading of bio-recognition molecule on the transducer surface, which in turn results in increased sensitivity of the biosensor. The immobilized phage particles retained their high infectivity towards host bacteria cells as confirmed by fluorescence microscopy. The biosensor was highly selective towards *E. coli* B strain with a reliable detection limit of 10^3 CFU/mL. Future studies would also focus on improving the performance of the biosensor by extending phage deposition time and increasing substrate surface area to obtain higher surface coverage of phages. Also a homogeneous electrode surface, for example, electrode with CNT directly grown on the surface, will definitely be helpful for uniform surface deposition, leading to oriented phage immobilization with minimal particle aggregation. The charge-directed immobilization method for bacteriophage attachment on CNT that has been developed in this work, could be widely applied for the developing of other type of biosensors and biological electrodes.

Acknowledgement

We would like to thank Dr. Yajun Yan for kindly providing the *E. coli K* strain. We also thank Dr. Jason Locklin's help with ATR-FTIR measurements and Dr. Hitesh Handa for the help with fluorescence imaging.

Supporting Information

Further details on phage propagation method; preparation of PEI-functionalized CNT; fluorescence imaging of bacteria and phage are available in the Supporting Information. Additional information as noted in text. This material is available free of charge via the Internet at http://pubs.acs.org.

References:

(1) *Estimates of Foodborne Illness in the United States, Centers for Disease Control and Prevention* **2011**.
(2) *Centers for Disease Control and Prevention* **2015**.
(3) *Health topics on Tuberculosis, World Health Organization* **2014**.
(4) Ahmed, A.; Rushworth, J. V.; Hirst, N. A.; Millner, P. A. *Clin. Microbiol. Rev.* **2014**, *27*, 631-646.
(5) Ivnitski, D.; Abdel-Hamid, I.; Atanasov, P.; Wilkins, E. *Biosensors Bioelectron.* **1999**, *14*, 599-624.
(6) Ivnitski, D.; Abdel-Hamid, I.; Atanasov, P.; Wilkins, E.; Stricker, S. *Electroanalysis* **1999**, *12*, 317-325.
(7) Setterington, E. B.; Alocilja, E. C. *Biosensors* **2012**, *2*, 15-21.
(8) Maalouf, R.; Fournier-Wirth, C.; Coste, J.; Chebib, H.; Saı1kali, Y.; Vittori, O.; Errachid, A.; Cloarec, J.-P.; Martelet, C.; Jaffrezic-Renault, N. *Analytical Chemistry (Washington, DC, United States)* **2007**, *79*, 4879-4886.
(9) Viswanathan, S.; Rani, C.; Ho, J.-a. A. *Talanta* **2012**, *94*, 315-319.
(10) BarreirosdosSantos, M.; J.P.Agusil; B.Prieto-Simo´n; C.Sporer; V.Teixeira; Samitier, J. *Biosensors Bioelectron.* **2013**, *45*, 174-180.
(11) Arya, S. K.; Singh, A.; Naidoo, R.; Wu, P.; McDermott, M. T.; Evoy, S. *Analyst* **2011**, *136*, 486-492.
(12) Edgar, R.; McKinstry, M.; Hwang, J.; Oppenheim, A. B.; Fekete, R. A.; Giulian, G.; Merril, C.; Nagashima, K.; Adhya, S. *Proc. Natl. Acad. Sci. USA* **2006**, *103*, 4841-4845.
(13) Stevens, K. A.; Jaykus, L. A. *Crit. Rev. Microbiol.* **2004**, *30*, 7-24.
(14) Nanduri, V.; Sorokulova, I. B.; Samoylov, A. M.; Simonian, A. L.; Petrenko, V. A.; Vodyanoy, V. *Biosensors Bioelectron.* **2007**, *22*, 986-992.
(15) Shabani, A.; Zourob, M.; Allain, B.; Marquette, C. A.; Lawrence, M. F.; Mandeville, R. *Anal. Chem.* **2008**, *80*, 9475-9482.
(16) Singh, A.; Glass, N.; Tolba, M.; Brovko, L.; Griffiths, M.; Evoy, S. *Biosensors Bioelectron.* **2009**, *24*, 3645-3651.
(17) Pearson, H. A.; Sahukhal, G. S.; Elasri, M. O.; Urban, M. W. *Biomacromolecules* **2013**, *14*, 1257-1261.
(18) Ahn, S.; Jeon, S.; Kwak, E.-A.; Kim, J.-M.; Jaworski, J. *Colloids Surf. B. Biointerfaces* **2014**, *122*, 851-856.
(19) Tolba, M.; Minikh, O.; Brovko, L. Y.; Evoy, S.; Griffiths, M. W. *Appl. Environ. Microbiol.* **2010**, *76*, 528-535.
(20) Hosseinidoust, Z.; Olsson, A. L.; Tufenkji, N. *Colloids Surf. B. Biointerfaces* **2014**, *124*, 2-16.
(21) Gervais, L.; Gel, M.; Allain, B.; Tolba, M.; Brovko, L.; Zourob, M.; Mandeville, R.; Griffiths, M.; Evoy, S. *Sensors and Actuators B* **2007**, *125*, 615-621.

(22) Hosseinidoust, Z.; Ven, T. G. M. V. d.; Tufenkji, N. *Langmuir* **2011**, *27*.
(23) Anany, H.; Chen, W.; Pelton, R.; Griffiths, M. W. *Appl. Environ. Microbiol.* **2011**, *77*, 6379-6387.
(24) Han, J.-H.; Wang, M. S.; Das, J.; Sudheendra, L.; Vonasek, E.; Nitin, N.; Kennedy, I. M. *ACS Applied materials and Interfaces* **2014**, *6*, 4758-4765.
(25) Richter, Ł.; Matuła, K.; Leśniewski, A.; Kwaśnicka, K.; Łoś, J.; Łoś, M.; Paczesny, J.; Hołyst, R. *Sensors Actuators B: Chem.* **2016**, *224*, 233-240.
(26) Li, R.; Wang, X.; Ji, Z.; Sun, B.; Zhang, H.; Chang, C. H.; Sijie Lin; Meng, H.; Liao, Y.-P.; Wang, M.; Li, Z.; Hwang, A. A.; Song, T.-B.; Xu, R.; Yang, Y.; Zink, J. I.; Ne, A. E.; Xia, T. *ACS Nano* **2013**, *3*, 2352-2368.
(27) Ramasamy, R. P.; Luckarift, H. R.; Ivnitski, D. M.; Atanassov, P. B.; Johnson, G. R. *Chem Commun (Camb)* **2010**, *46*, 6045-6047.
(28) Lau, C.; Adkins, E. R.; Ramasamy, R. P.; Luckarift, H. R.; Johnson, G. R.; Atanassov, P. *Advanced Energy Materials* **2012**, *2*, 162-168.
(29) Parimi, N. S.; Umasankar, Y.; Atanassov, P.; Ramasamy, R. P. *ACS Catalysis* **2012**, *2*, 38-44.
(30) Calkins, J. O.; Umasankar, Y.; O'Neill, H.; Ramasamy, R. P. *Energy & Environmental Science* **2013**, *6*, 1891-1900.
(31) Sekar, N.; Umasankar, Y.; Ramasamy, R. P. *Phys. Chem. Chem. Phys.* **2014**, *16*, 7862-7871.
(32) Van Valen, D.; Wu, D.; Chen, Y. J.; Tuson, H.; Wiggins, P.; Phillips, R. *Curr. Biol.* **2012**, *22*, 1339-1343.
(33) Ovesny, M.; Krizek, P.; Borkovec, J.; Svindrych, Z.; Hagen, G. M. *Bioinformatics* **2014**, *30*, 2389-2390.
(34) Andrews, J. M.; Testing, B. W. P. o. S. *J. Antimicrob. Chemother.* **2009**, *64*, 454-489.
(35) Zhang, G.; Dang, L.; Li, L.; Wang, R.; Fu, H.; Shi, K. *CrystEngComm* **2013**, *15*, 4730.
(36) Umasankar, Y.; Ramasamy, R. P. *Catalysis Science & Technology* **2013**, *3*, 2546-2549.
(37) Zhou, Y.; Umasankar, Y.; Ramasamy, R. P. *J. Electrochem. Soc.* **2015**, *162*, H911-H917.
(38) Sadeghi, G.; Schijven, J. F.; Behrends, T.; Hassanizadeh, S. M.; Gerritse, J.; Kleingeld, P. J. *Ground Water* **2011**, *49*, 12-19.
(39) Zweckstetter, M.; Hummer, G.; Bax, A. *Biophys. J.* **2004**, *86*, 3444-3460.
(40) Zhou, B.; Lin, Y.; Harruff, B. A.; Sun, Y.-P. *Photoluminescence Properties of Carbon Nanotubes*; Springer-Verlag Berlin Heidelberg, 2008; Vol. 4.
(41) Tlili, C.; Sokullu, E.; Safavieh, M.; Tolba, M.; Ahmed, M. U.; Zourob, M. *Anal. Chem.* **2013**, *85*, 4893-4901.
(42) Shabani, A.; Marquette, C. A.; Mandeville, R.; Lawrence, M. F. *Analyst* **2013**, *138*, 1434-1440.
(43) Bekir, K.; Barhoumi, H.; Braiek, M.; Chrouda, A.; Zine, N.; Abid, N.; Maaref, A.; Bakhrouf, A.; Ouada, H. B.; Jaffrezic-Renault, N.; Mansour, H. B. *Environ Sci Pollut Res* **2015**, *22*, 15796-15803.
(44) Li, Y.; Afrasiabi, R.; Fathi, F.; Wang, N.; Xiang, C.; RyanLove; She, Z.; Kraatz, H.-B.

Biosensors Bioelectron. **2014**, *58*, 193-199.
(45) Mejri, M. B.; Baccar, H.; Baldrich, E.; Del Campo, F. J.; Helali, S.; Ktari, T.; Simonian, A.; Aouni, M.; Abdelghani, A. *Biosens. Bioelectron.* **2010**, *26*, 1261-1267.
(46) Long, G. L.; Winefordner, J. D. *Anal. Chem.* **1983**, *55*, 712-724.

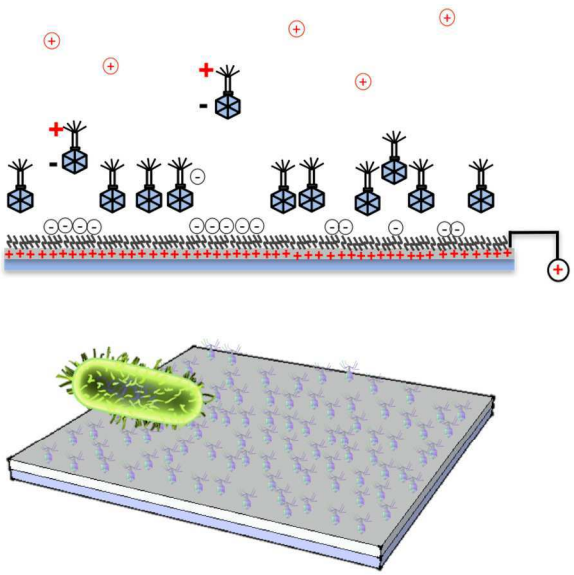

Scheme 1. Schematic description of the charge-directed orientation and immobilization of bacteriophage onto PEI-functionalized CNT on electrode surface.

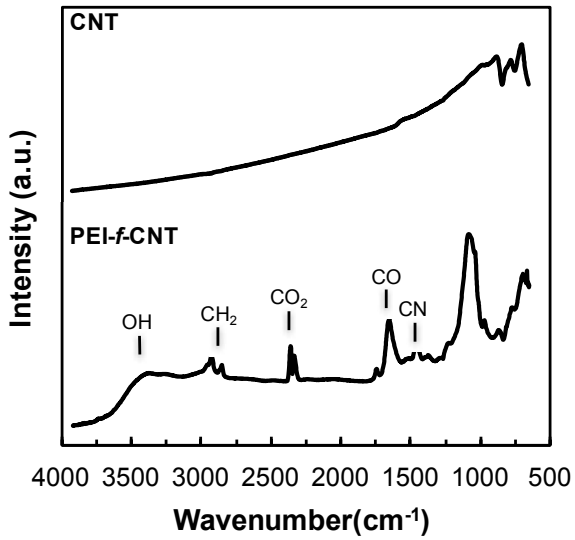

Figure 1. ATR-FTIR spectra of unmodified and PEI-*f*-CNT.

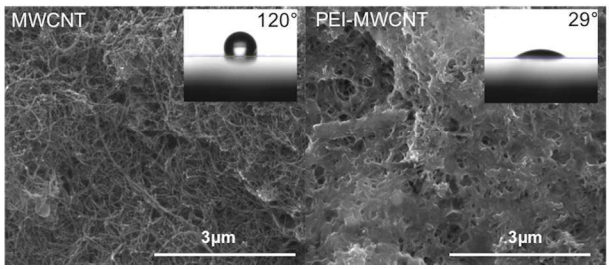

Figure 2. SEM images of CNT before and after PEI modification. Inset: Images of water droplet on the substrates and their contact angles

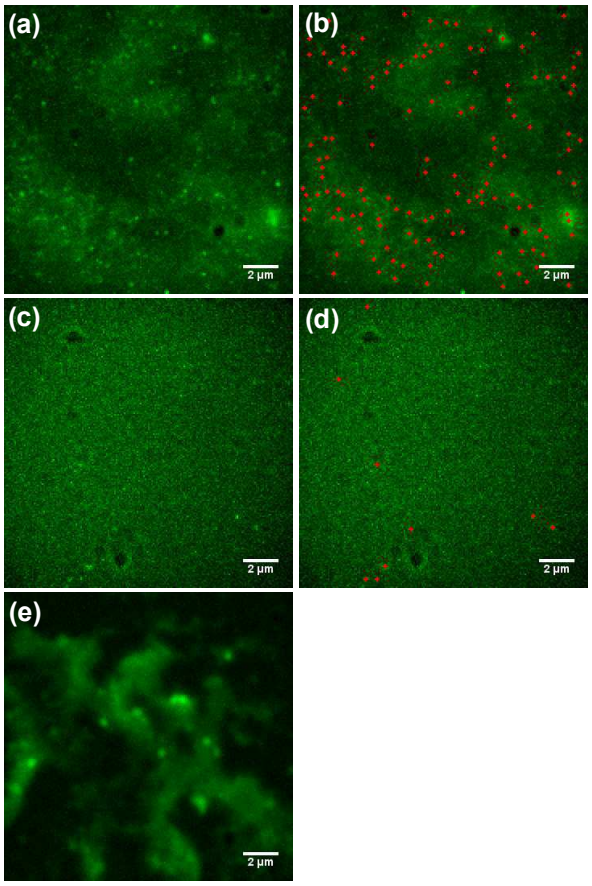

Figure 3. Fluorescence images of: (a-b) Surface immobilized phage particles by electric field-induced covalent immobilization; (c-d) Surface immobilized phage particles by covalent immobilization without applying electric field; (e) CNT surface in the absence of phage particles. (b) and (d) are the same images as that of (a) and (c) with the phages highlighted in red color. 140 phage particles were detected in (a), and 9 were detected in (b) using the method described above. The laser power was 114 W/cm^2 for images (a-d) and 343 W/cm^2 for images (e).

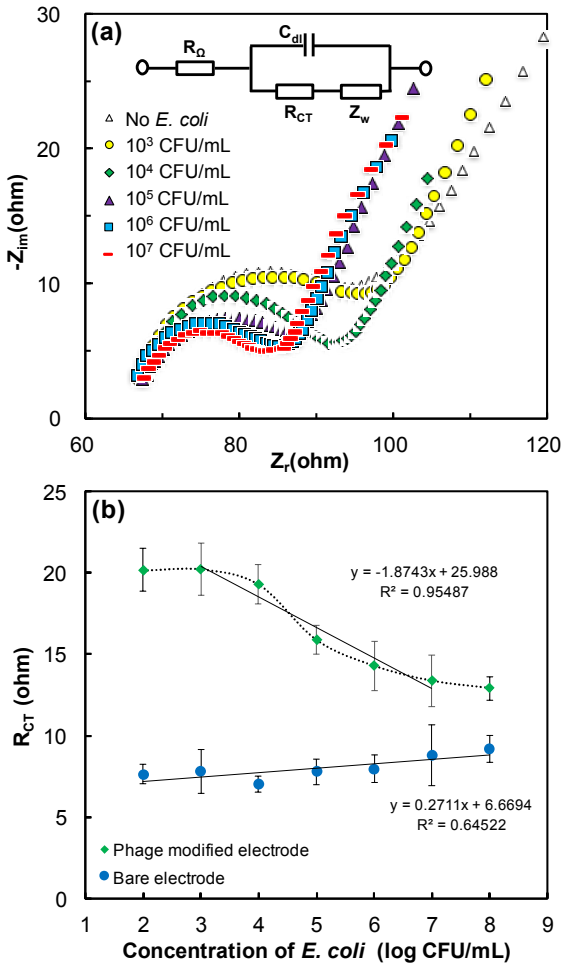

Figure 4. (a) Nyquist plot for T2-modified electrode in the absence and presence of *E. coli* B at different concentrations. (Inset: Randles equivalent circuit); (b) Variations of charge transfer resistance at different *E. coli* B concentrations with phage modified electrodes and bare electrode.

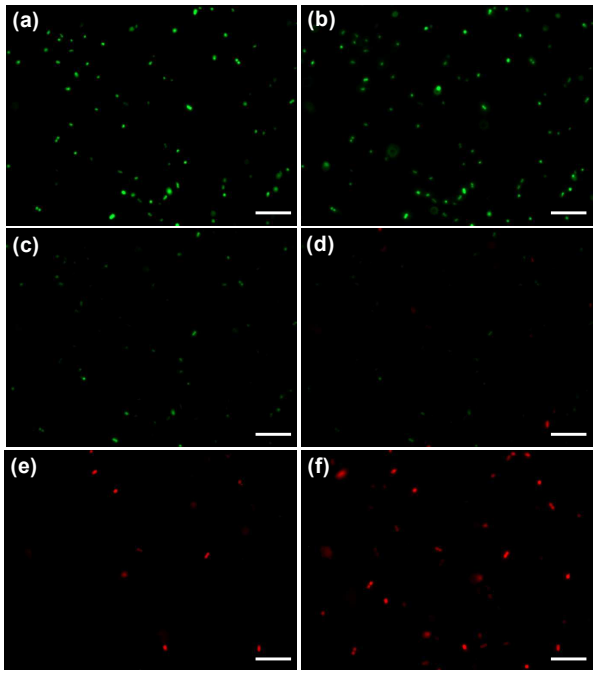

Figure 5. Representative images of bacterial cell lysis monitored by fluorescence microscope using the Backlight bacteria viability kit. (a) 10 min; (b) 15 min; (c) 20 min; (d) 25 min; (e) 30 min; (f) 35 min. Green dots represent live bacteria, and red dots represent lysed bacteria. The scale bar is 10 μm.

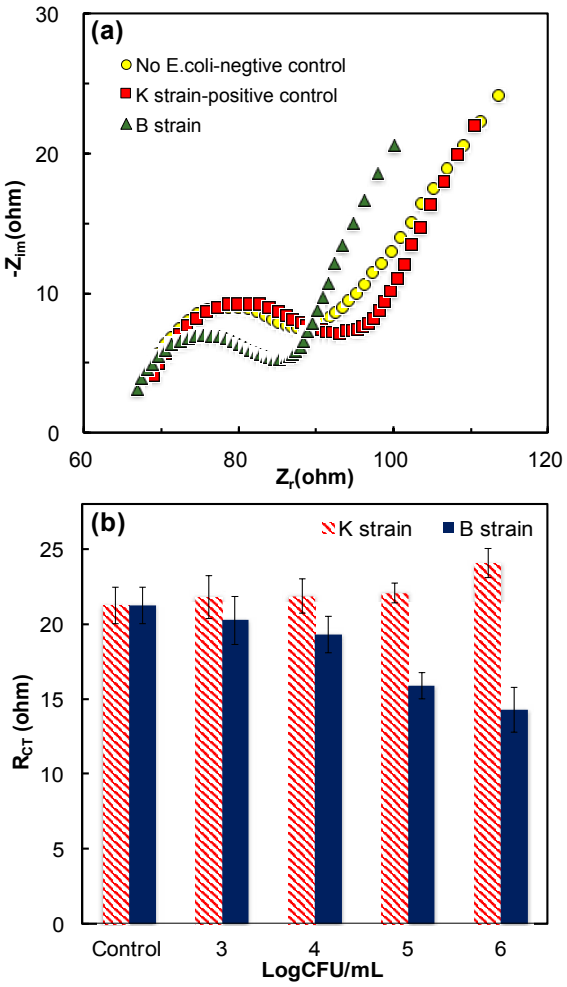

Figure 6. (a) Nyquist plot of T2-modified electrode in the absence and presence (10^6 CFU/mL) of native host (B strain) and non-host (K strain) *E. coli*. (b) Variation of R_{CT} with increasing bacterial concentrations for B and K strains of *E. coli*. (Values are the average of 3 replicates).

For TOC only: